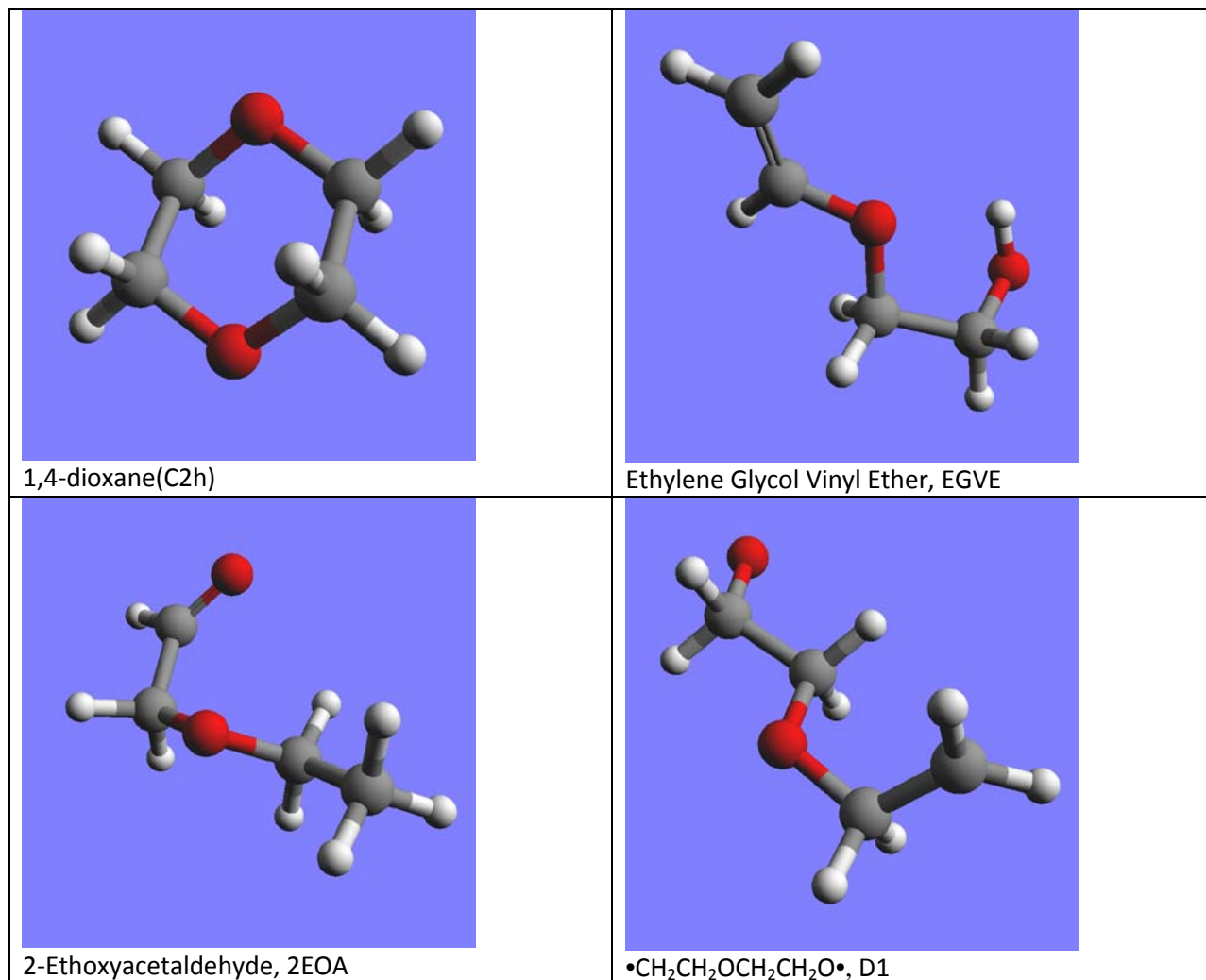


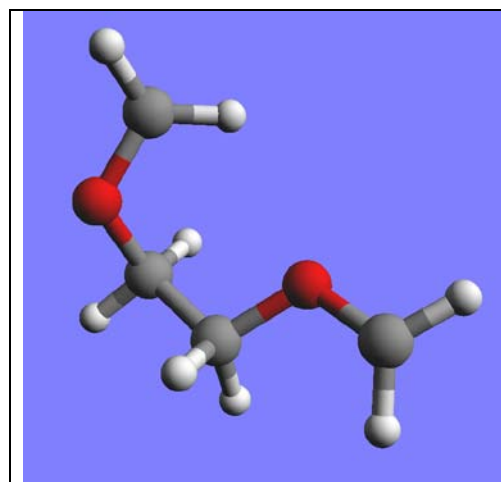
A shock tube and theoretical study on the pyrolysis of 1,4-dioxane

Authors: *X. Yang, A. W. Jasper, B. R. Giri, J. H. Kiefer and R. S. Tranter*

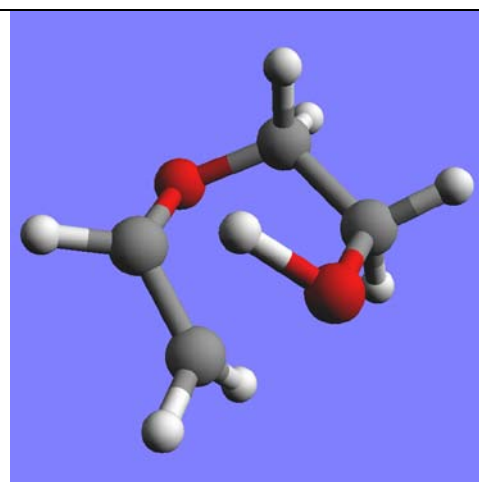
Supplementary information Table S1: Structures of 1,4-Dioxane, intermediates and transition states calculated using multireference method

CASPT2/CBS//CASPT2/aug-cc-pVDZ, labels are from Table I

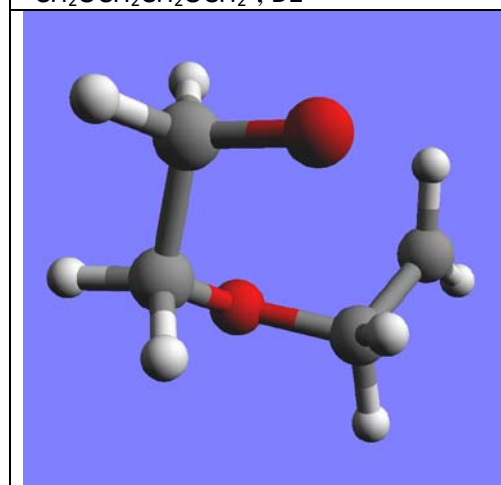




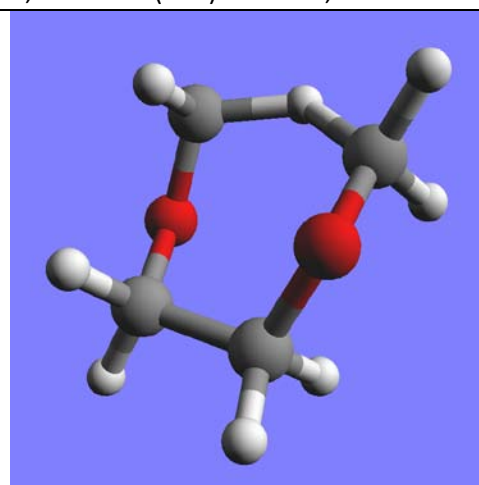
$\bullet\text{CH}_2\text{OCH}_2\text{CH}_2\text{OCH}_2^+$, D2



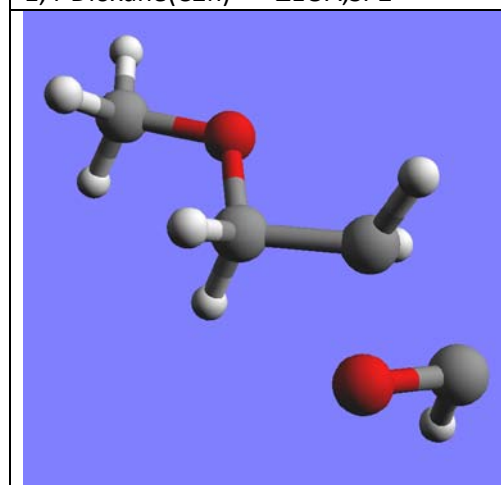
1,4-Dioxane(C2h) \rightarrow EGVE, SP1



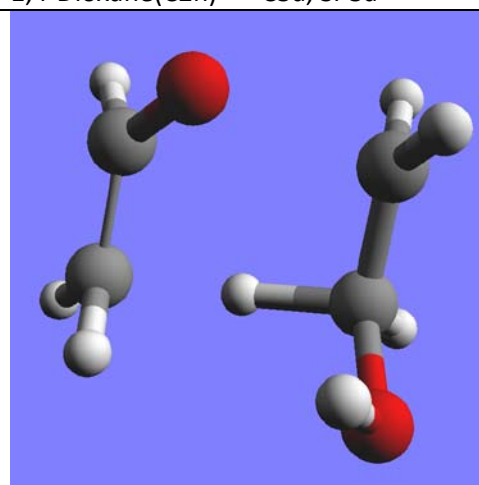
1,4-Dioxane(C2h) \rightarrow 2EOA, SP2



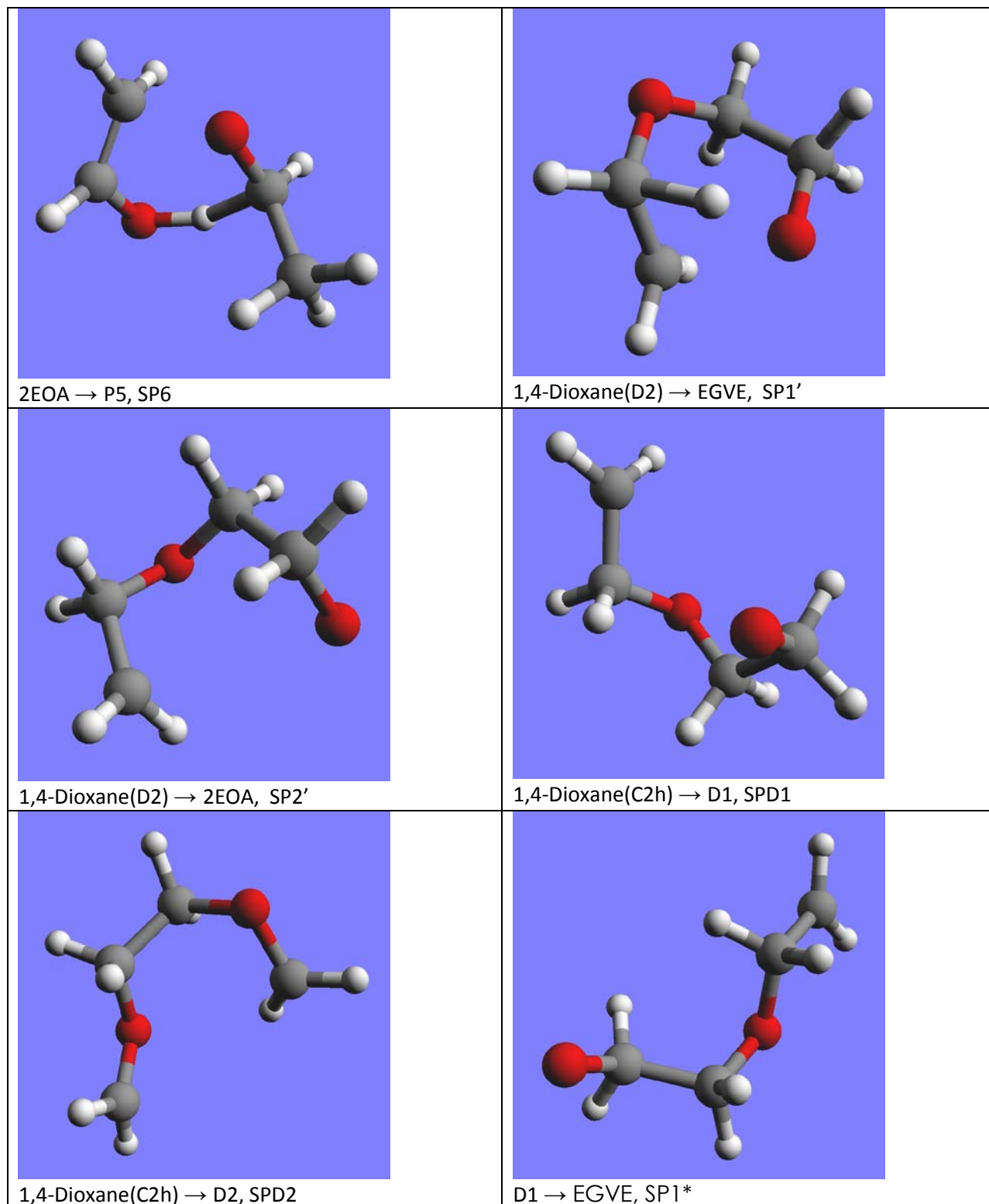
1,4-Dioxane(C2h) \rightarrow C3a, SP3a

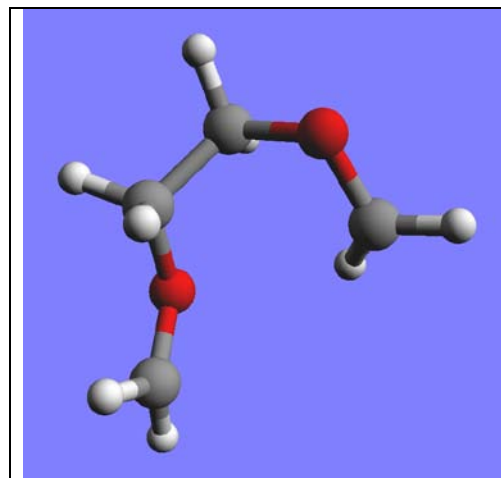


C3a \rightarrow MOP, SP3b

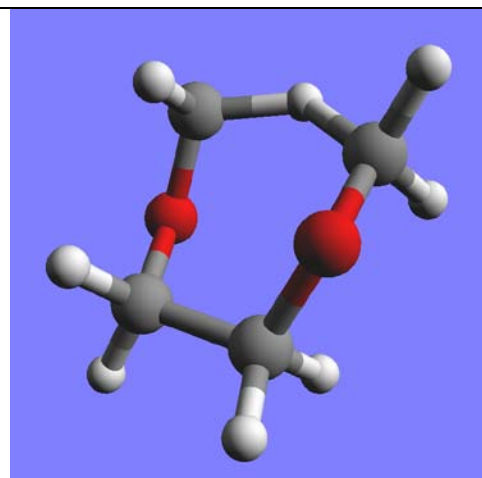


EGVE \rightarrow P5, SP5





D1 → 2EOA, SP1*



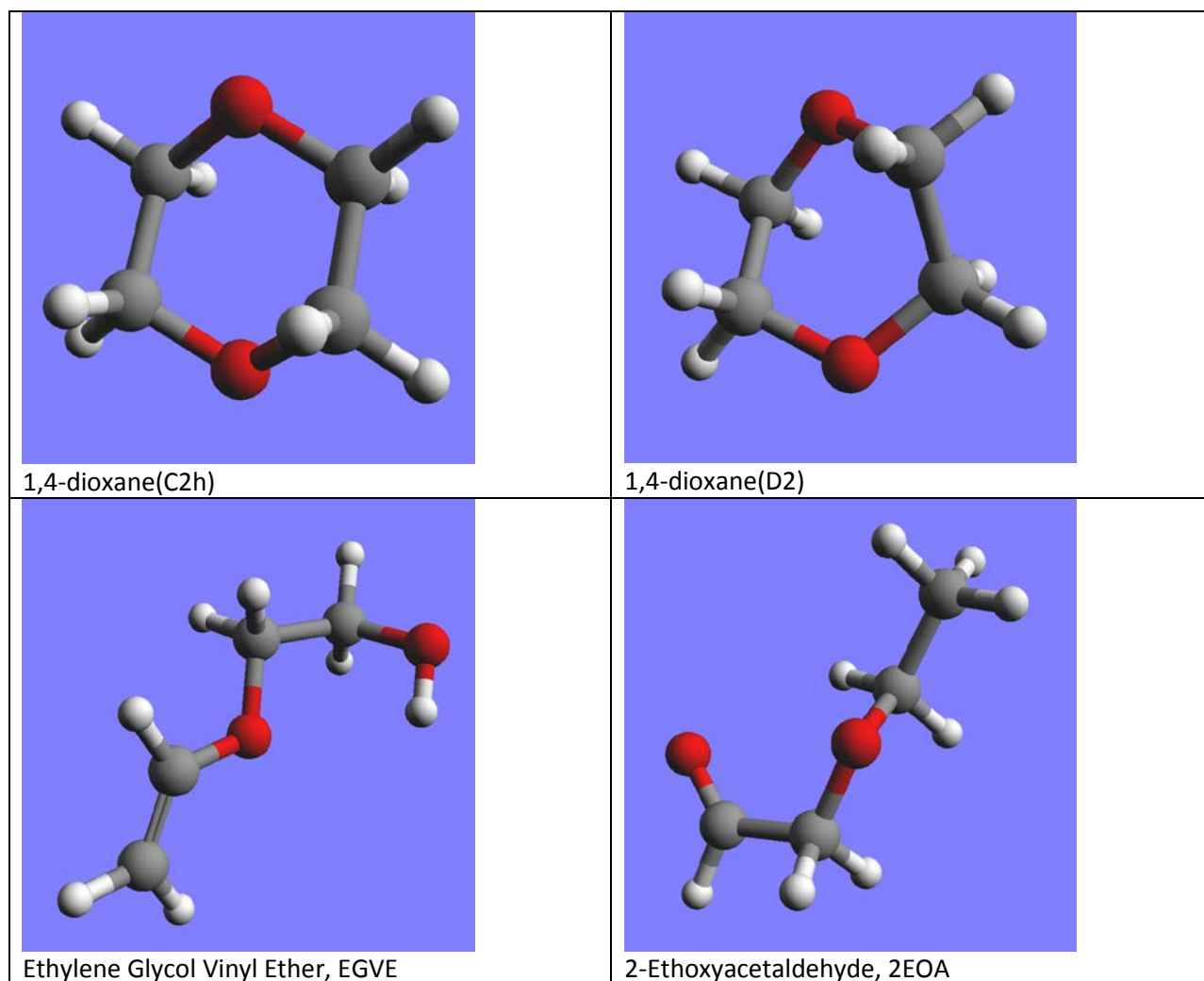
D2 → C3d, SP3a*

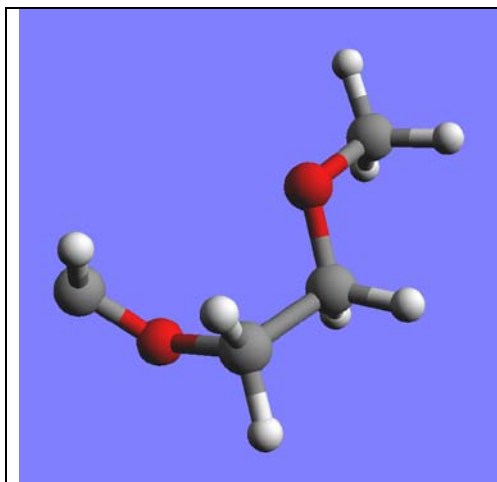
A shock tube and theoretical study on the pyrolysis of 1,4-dioxane

Authors: *X. Yang, A. W. Jasper, B. R. Giri, J. H. Kiefer and R. S. Tranter*

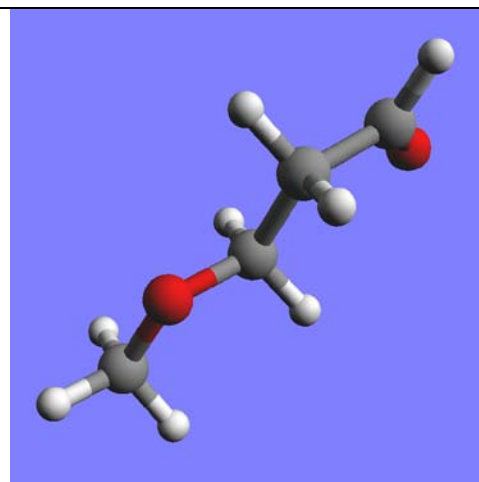
Supplementary information Table S2: Structures of 1,4-Dioxane, intermediates and transition states calculated using single reference method

QCISD(T)/CBS//B3LYP/6-311++G(d,p), labels are from Table I

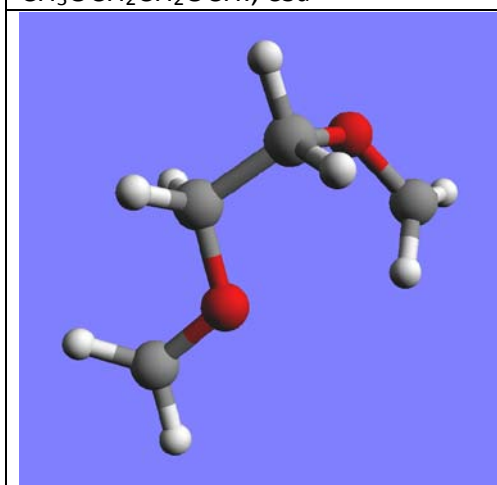




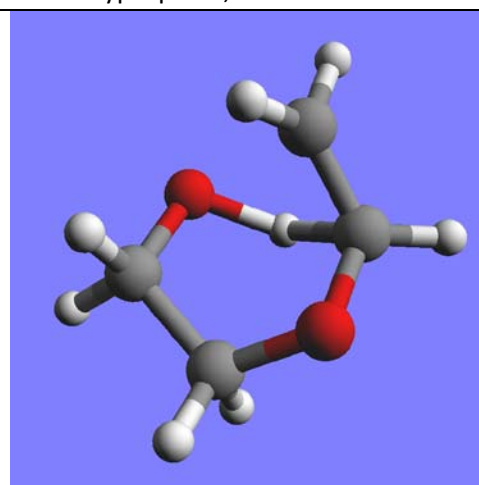
CH₃OCH₂CH₂OCH₃, C3a



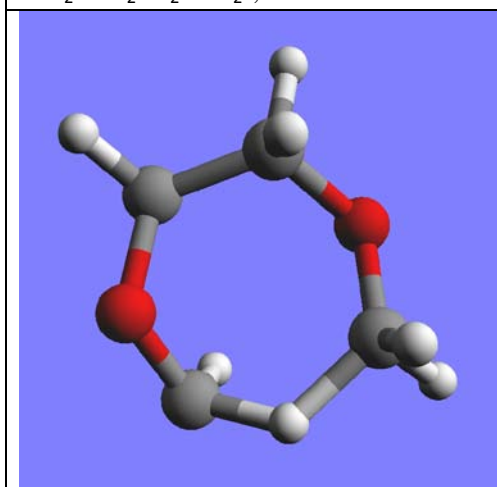
Methoxypropanal, MOP



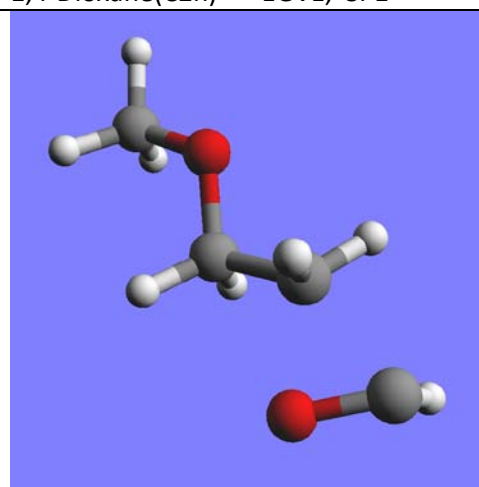
•CH₂OCH₂CH₂OCH₂•, D2



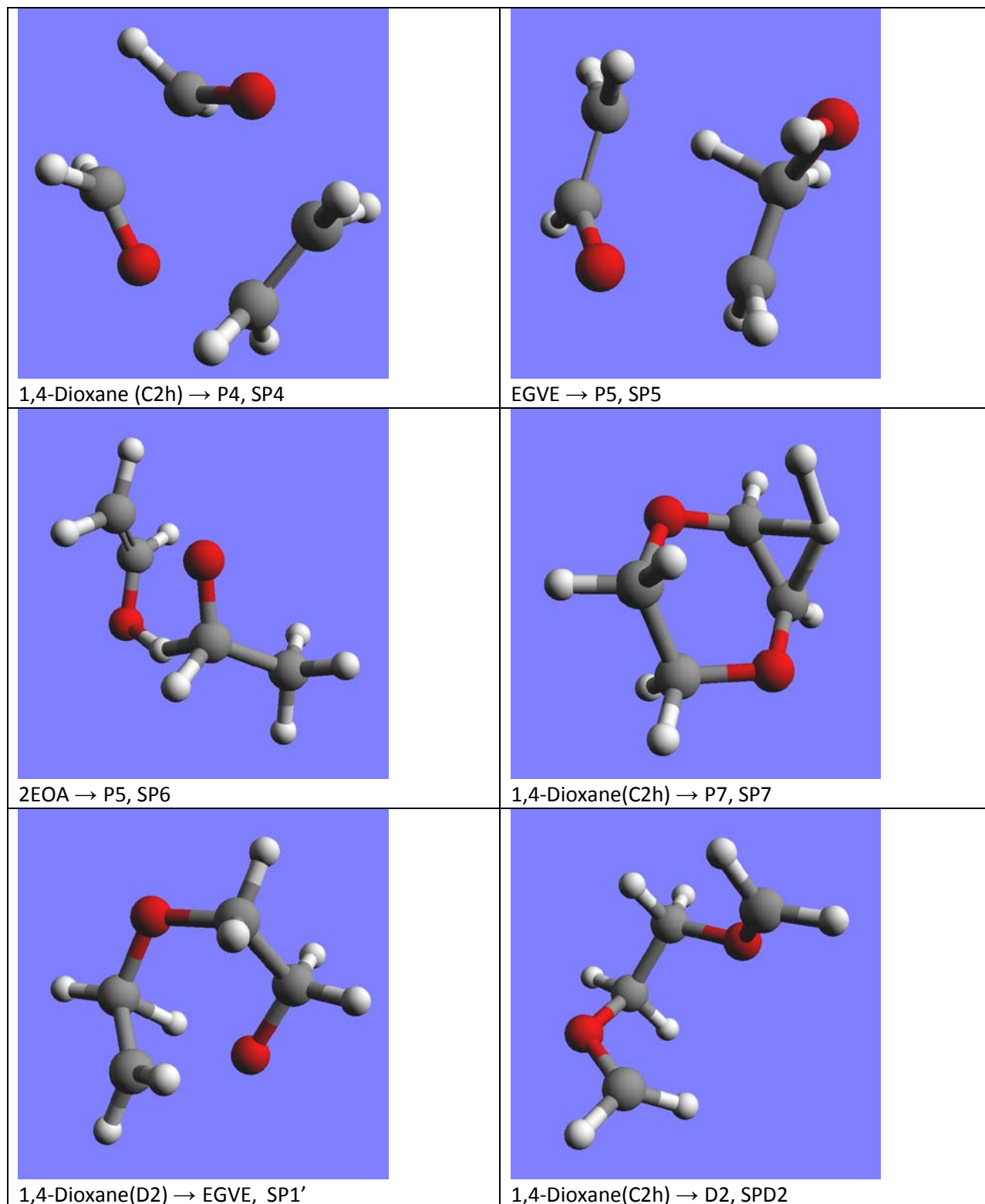
1,4-Dioxane(C_{2h}) → EGVE, SP1

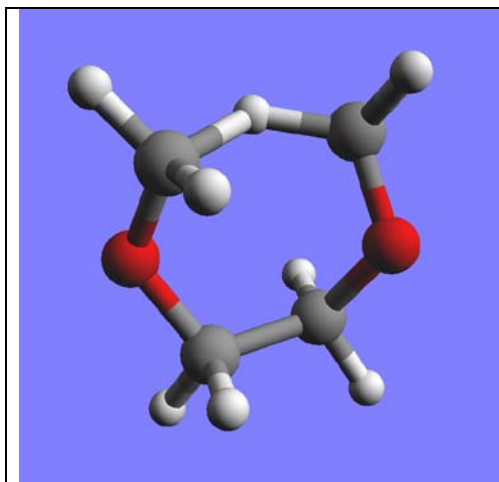


1,4-Dioxane(C_{2h}) → C3a, SP3a



C3a → MOP, SP3b





D2 → C3d, SP3a*

A shock tube and theoretical study on the pyrolysis of 1,4-dioxane

Authors: *X. Yang, A. W. Jasper, B. R. Giri, J. H. Kiefer and R. S. Tranter*

Supplementary information S4

Master equation calculations

The ring opening kinetics of 1,4-dioxane was studied using the master equation (ME) formulation of Miller and Klippensteinⁱ and the computer code VariFlex.ⁱⁱ The fluxes through the saddle points were calculated using rigid rotor/harmonic oscillator (RRHO) transition state theory. Tunneling and variational effects were considered and found to have a small effect on the predicted kinetics. The stepwise kinetics of ring opening via the diradical intermediates was modeled using unified statistical theory^{iii,iv} (UST); the effect of the SPD1 saddle point and the diradical intermediate on the fluxes through the SP1* and SP2* pathways was included using a variant of UST generalized to handle branching to multiple products. Both the C_{2h} and D₂ conformers of dioxane and their low-lying transition state for interconversion were included in the ME calculation. The C_{2h} and D₂ conformers were treated as a unified species to improve the numerical stability of the calculated kinetics; this is a feature of VariFlex recently developed and implemented by Klippenstein and Miller.^v The exponential down model was used to treat collisional energy transfer for the bath gas Kr, where the average downward energy transfer parameter α was empirically adjusted to best fit the experimental data. Seven decomposition pathways were included in the ME calculations: SP1, SP1', SP1*, SP2, SP2', SP2*, and SP3a* (see Fig. 5b from the article). The saddle point energies for these processes were taken from the composite single reference/multireference potential energy surface presented in Table 1 and Fig. 5 of the article.

Ring opening via SP3a* was found to be negligible (~0.2%), and this process is not considered further. The predicted rates for the formation of EGVE (k_1) and the formation of 2EOA (k_2) are shown in Fig. S1(a) with α empirically adjusted to 550 cm⁻¹. The agreement between the theoretical and experimental rate coefficients is fair but not quantitative. As discussed in the text, the loose nature of the diradical transition states likely contributes significant error to the predicted kinetics. To improve agreement with the experimental results

and to approximate the effect of anharmonicities at the loose transition states, the harmonic frequencies for the SP2' were scaled by 1.05 and the harmonic frequencies for SP1* and SP2* were scaled by 0.95. The energy transfer parameter α was reoptimized to 450 cm⁻¹. The resulting rate coefficients (shown in Fig. S1(b)) are in much better agreement with the experimental results, although the temperature dependence of the theoretical prediction is still somewhat stronger than that of the experimental results. In another set of sensitivity tests, we found that a wide range of branching ratios could be obtained by making small adjustments (~1 kcal/mol) to the relative barrier heights for ring opening, with values for $k_1/(k_1+k_2)$ ranging from 20–80%. These sensitivity tests of the predicted kinetics to reasonable adjustments in the various theoretical parameters demonstrate how errors in the harmonic evaluations of the densities of states and uncertainties in the energy transfer models and thermochemistry likely preclude a quantitative or semi-quantitative theoretical prediction for this system. Further quantitative refinement of the ME model was not pursued.

As discussed above, the EGVE and 2EOA intermediates can be formed via several pathways: directly from dioxane via SP1 and SP2, directly from the higher-energy twist conformer of dioxane via SP1' and SP2', and via a diradical intermediate and the SP1* and SP2* saddle points. In Fig. S2, the contributions to the total rates of formation of EGVE and 2EOA from each of these pathway are shown for the empirically adjusted ME calculations. Five of the six pathways (all but SP1') contribute significantly to the overall decomposition of dioxane.

Modified Arrhenius expressions for 1500–2200 K fit to k_1 and k_2 for the empirically adjusted model shown in Fig. S1(b) are provided:

$$\begin{aligned}k_{1,\infty}(T) &= 4.703 \times 10^{15} (T/298 \text{ K})^{1.123} \exp(-41517 \text{ K}/T) \text{ s}^{-1} \\k_{2,\infty}(T) &= 3.365 \times 10^{17} (T/298 \text{ K})^{-0.3375} \exp(-43807 \text{ K}/T) \text{ s}^{-1} \\k_{1,60\text{Torr}}(T) &= 2.529 \times 10^{27} (T/298 \text{ K})^{-14.83} \exp(-47217 \text{ K}/T) \text{ s}^{-1} \\k_{2,60\text{Torr}}(T) &= 1.594 \times 10^{28} (T/298 \text{ K})^{-15.32} \exp(-48489 \text{ K}/T) \text{ s}^{-1} \\k_{1,120\text{Torr}}(T) &= 1.884 \times 10^{29} (T/298 \text{ K})^{-16.04} \exp(-50234 \text{ K}/T) \text{ s}^{-1} \\k_{2,120\text{Torr}}(T) &= 1.236 \times 10^{30} (T/298 \text{ K})^{-16.54} \exp(-51486 \text{ K}/T) \text{ s}^{-1}\end{aligned}$$

These expressions likely have large uncertainties.

Figure S1

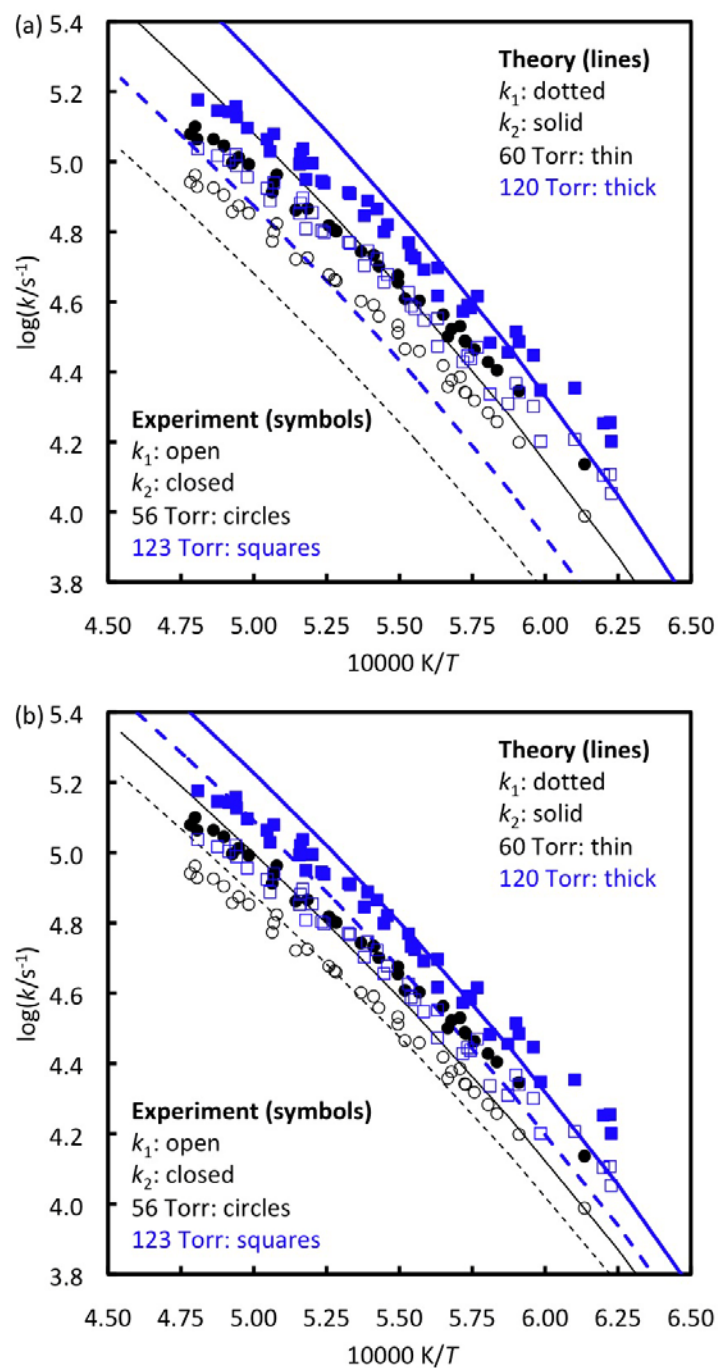


Fig. S1. Total rate coefficients for the formation of EGVE (k_1) and 2EOA (k_2) obtained from experiment and from theory. An unmodified RRHO treatment for the transition state fluxes was employed in panel (a). In panel (b) the harmonic frequencies were empirically scaled when calculating the fluxes through the loose saddle points to approximately account for anharmonicity.

Figure S2

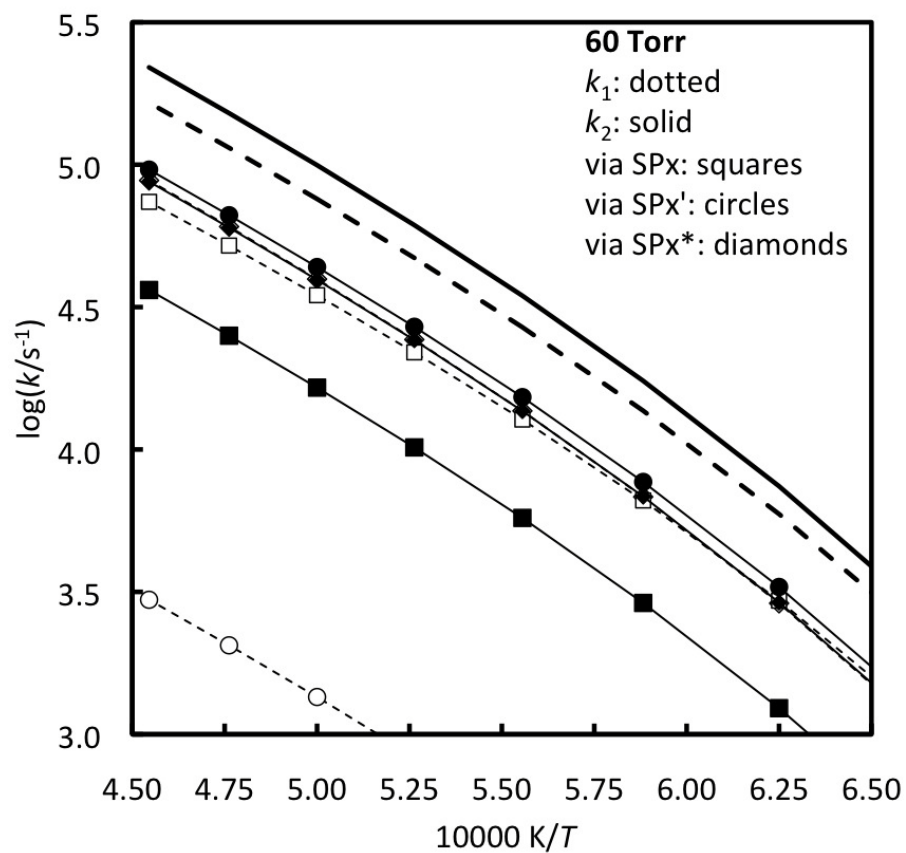


Fig. S2. Contributions from several ring opening pathways to the predicted total rate coefficients for the formation of EGVE (k_1) and 2EOA (k_2) at 60 Torr. The rate coefficients for the two diradical pathways (diamonds) are similar and difficult to distinguish in the figure.

References

- ⁱ Miller, J. A.; Klippenstein, S. J. *J. Phys. Chem. A* **2006**, *110* (36), 10528-10544.
- ⁱⁱ Klippenstein, S. J.; Wagner, A. F.; Dunbar, R. C.; Wardlaw, D. M.; Robertson, S. H.; Miller, J. A.; Harding, L. B. Variflex, version 2.0. *Argonne National Laboratory* **2010**.
- ⁱⁱⁱ Miller, W. H. *J. Chem. Phys.* **1976**, *65* (6), 2216-2223.
- ^{iv} Klippenstein, S. J.; Khundkar, L. R.; Zewail, A. H.; Marcus, R. A. *J. Chem. Phys.* **1988**, *89* (8), 4761-4770.
- ^v Miller, J. A.; Klippenstein, S. J., private communication, 2010.